HHS Public Access

Author manuscript

Mol Imaging Biol. Author manuscript; available in PMC 2021 October 01.

Published in final edited form as:

Mol Imaging Biol. 2020 October ; 22(5): 1403–1413. doi:10.1007/s11307-020-01520-w.

Cross-species physiological assessment of brain estrogen receptor expression using ^{18}F-FES and ^{18}F-4FMFES PET imaging

Michel Paquette[1,2], **Serge Phoenix**[1,2], **Éric Lavallée**[2], **Jacques A Rousseau**[1,2], **Brigitte Guérin**[1,2], **Éric E Turcotte**[1,2], **Roger Lecomte**[1,2]

[1.]Department of Nuclear Medicine and Radiobiology, Faculty of Medicine and Health Sciences, Université deSherbrooke, Sherbrooke, QC, Canada

[2.]Sherbrooke Molecular Imaging Center, Centre de Recherche du Centre Hospitalier Universitaire de Sherbrooke (CRCHUS), Sherbrooke, QC, Canada.

Abstract

Purpose: A retrospective analysis was performed of preclinical and clinical data acquired during the evaluation of the estrogen receptor (ER) PET tracer 4-fluoro-11β-methoxy-16α-[^{18}F]-fluoroestradiol (4FMFES) and its comparison with 16α-[^{18}F]-fluoroestradiol (FES) in mice, rats and humans with a focus on the brain uptake.

Procedures: Breast cancer tumor-bearing female BALB/c mice from a previous study and female Sprague-Dawley rats (control and ovariectomized) were imaged by 4FMFES or FES-PET imaging. Immediately after, low-dose CT was performed in the same bed position. Semi-quantitative analysis was conducted to extract %ID/g data. Small cohorts of mice and rats were imaged with 4FMFES in an ultra-high-resolution small animal PET scanner prototype (LabPET II). Rat brains were dissected and imaged separately with both PET and autoradiography. In parallel, 31 breast cancer patients were enrolled in a clinical phase II study to compare 4FMFES with FES for oncological assessment. Since the head was included in the field-of-view, brain uptake of discernable foci was measured and reported as SUV_{Max}.

Results: Regardless of the species studied, 4FMFES and FES uptake was relatively uniform in most regions of the brain, except for bilateral foci at the base of the skull, at the midsection of the brain. Anatomical localization of the PET signal using CT image fusion indicates that the signal origins from the pituitary in all studied species. 4FMFES yielded lower pituitary uptake than FES in patients, but an inverse trend was observed in rodents. 4FMFES pituitary contrast was higher than FES in all assessed groups. High-resolution small animal imaging of the brain of rats and mice revealed a supplemental signal anterior to the pituitary, which is likely to be the medial

Corresponding author: Michel Paquette, PhD, CIMS/CRCHUS, 3001, 12th Avenue N, Sherbrooke, Qc, Canada, Tel: (819)346-1110 x11982, Fax: (819)829-3238, Michel.Paquette@Usherbrooke.ca.

Conflicts of interest/Competing interests: RL is a co-founder and chief scientific officer of IR&T Inc. who was involved in the development of the prototype ultra-high-resolution PET scanner LabPET II. The other authors have no conflict of interest to declare regarding this paper or the results therein.

Compliance with ethical standards: All animal procedures were approved by the Ethical Committee for Animal Care of the Université de Sherbrooke, in compliance with the policies and directives of the Canadian Council on Animal Care. Patients were retroactively analysed from a previously reported phase II breast cancer clinical trial evaluating 4FMFES-PET, which was performed under the authority of Health Canada and approved by the Sherbrooke University Hospital Clinical Research Ethics Committee and Institutional Board.

preoptic area. Dissection data further confirmed those findings and revealed additional signals corresponding to the arcuate and ventromedial nuclei, along with the medial and cortical amygdala.

Conclusion: 4FMFES allowed visualization of ER expression in the pituitary in humans and two different rodent species with better contrast than FES. Improvement in clinical spatial resolution might allow visualization and analysis of other ER-rich brain areas in humans. Further work is now possible to link 4FMFES pituitary uptake to cognitive functions.

Keywords

Estrogen Receptor; Brain PET; FES; 4FMFES

Introduction

The estrogen receptor (ER) is expressed in a wide array of tissues and mediates a plethora of important physiological roles [1]. The brain has many localized sites of variable ERα and ERβ expression [2], foretelling the crucial role estrogen-mediated signaling might have on behavior [3,4]. Indeed, concentration and memory impairments that occur in aging women were linked to menopause, suggesting a relationship between cognition and physiological estrogen stimulation [5–7]. Notably, two out of three Alzheimer's patients are women, making female sex the second most important factor after age for this disease [8], with the onset of menopause likely to play a role because of the drastic drop in estrogen levels [9]. Early age menopause [9] and oophorectomy [10] are linked with higher chance of developing dementia (including Alzheimer's), whereas hormone therapy initiated early post-menopause produced mixed results regarding long-term neuroprotection [11, 12]. Moreover, estradiol was shown to modulate a wide variety of genes linked to diverse functions such as lipid metabolism, vasodilatation and vasoconstriction, long term synaptic potentiation and myelination in the mouse cerebral cortex [13,14]. Hence, follow-up of the estrogen receptor (ER) in the brain would be of great interest to investigate the fundamental relationship between brain ER expression, aging and cognition. Previous *ex vivo* studies showed variable ER mRNA expression [15], anti-ER immunohistology [16] or estradiol-derived radiotracer uptake [17] in different portions of the brain. While there are many *in vitro* and *ex vivo* tools to investigate ER expression and estradiol binding, methods to assess and follow estrogen action and its spatiotemporal distribution in the brain *in vivo* are still lacking or perfectible.

The most advanced *in vivo* investigational tool for ER so far is PET imaging using ER radiotracers such as 16α-fluoroestradiol (FES) [18] or 4-fluoro-11β-methoxy-16α-[^{18}F]-fluoroestradiol (4FMFES) [19]. FES-PET was primarily and successfully used in numerous studies to assess ER status in breast cancer, both in the preclinical [20] and the clinical settings [21,22]. Extensive pharmacological evaluations validated the ER-binding properties of FES, and excellent correlations between tumor ER expression levels and FES uptake were observed. While brain studies using FES are scarcer than for oncology, previous work explored its binding pattern. Tissue slice analysis in rats demonstrated weak FES uptake in the hypothalamus and even weaker signal in a few other regions such as the preoptic area, the striatum and the amygdala [23]. A FES-PET/MRI study in female rats revealed the pituitary as the only cerebral structure showing discernable tracer uptake [24], which

corroborated earlier findings where dissected pituitary produced by far the highest FES accumulation [25].

In this work, in order to evaluate the uptake pattern of the ER PET tracers FES and 4FMFES in the brain of rodents and humans, we performed a retrospective analysis of preclinical and clinical data during comparison of those two tracers in tumor-bearing mice [26] and breast cancer patients [27], with a focus on the brain uptake and localization. Similarly, different cohorts of female rats were imaged with both tracers, allowing cross-species comparisons of brain uptake of both ER-targeting PET tracers. Moreover, to mimic menopausal condition and its effects on ER expression, we evaluated the brain uptake of ovariectomized and normal female rats with FES-PET. Finally, high-resolution images of rat and mouse brains were obtained using a small animal PET prototype (LabPET II) achieving a resolution of 0.74 mm FWHM [28].

Materials and methods

Radiochemistry

The methods used for the synthesis of FES have been previously reported [29]. The precursor for 4FMFES was synthesized as previously described [30]. Labeling at the 16α-position was accomplished via nucleophilic substitution on the 16β,17β-cyclic sulfate intermediate [19] using an optimized automated procedure [29]. Molar activity for 4FMFES ranged between 20 and 123 GBq/μmol, whereas it fluctuated between 90 and 251 GBq/μmol for FES.

Patient characteristics

Female breast cancer patients (n = 31) were recruited during a phase II trial aiming to compare tumor detection properties of both FES and 4FMFES, as described in our previous work [27]. Of those, 9 were pre-menopausal, and 22 were post-menopausal. Hormone therapy concomitant to imaging was among the exclusion factor for this study. Since PET scans were performed from thigh to apex, the whole brain was included in all acquisitions and thus was available for visualization and analysis.

Animal studies

Like what was done in the clinical study, a retrospective analysis of the brain region of a group of tumor-bearing BALB/c mice (n = 8) imaged sequentially with both FES and 4FMFES was performed [26]. Even if tumors were the main topic of interest in this study and were centered in the field-of-view, the head of those mice was fully included in the axial field of the PET scanners. Similarly, a cohort of female rats (n = 3) was imaged with both FES and 4FMFES-PET. Groups of female mice (n = 6) and female rats (n = 3) were used in a separate experiment and injected with 4FMFES to assess the resolving performance of the tiny cerebral structures expressing ER using a novel ultra-high-resolution small animal PET scanner prototype (LabPET II) [28].

In another investigation, 2 groups of female rats (control and ovariectomized; n = 3 each) were imaged with FES-PET to verify if brain uptake could be influenced by physiological

estrogen production and pharmacological action. Another group of female rats (n = 3) were imaged with 4FMFES twice within a week, the second imaging session was performed with co-injection of 100 μg estradiol. All animal procedures were approved by the Ethical Committee for Animal Care of the Université de Sherbrooke, in compliance with the policies and directives of the Canadian Council on Animal Care.

PET imaging

Patients and tumor-bearing mice PET/CT acquisitions were obtained from previous studies and thus were performed as described in their respective articles [26,27]. Patients were injected with 189.5 ± 17.5 MBq FES or 189.4 ± 11.8 MBq 4FMFES, whereas mice received either 4.5 ± 1.2 MBq FES or 10.5 ± 2.3 MBq 4FMFES. In both cases, subjects were injected with FES and 4FMFES in a random order. Mice were imaged with both tracers within a maximum of 1 week, whereas patients received their imaging sequence within an interval of 2 weeks. Cohorts of control and ovariectomized female rats were anesthetized with a 1.5% isoflurane – 2 L/min oxygen mixture, injected with 11.3 ± 0.5 MBq FES, then imaged 45 minutes later using a LabPET8/Triumph PET/CT platform.

To further investigate the resolving power of PET imaging, cohorts of anesthetized female mice and rats were injected with 12.5 ± 1.2 MBq of 4FMFES and imaged using the prototype LabPET II scanner, reaching 0.74 mm FWHM spatial resolution (0.4 μL volumetric resolution) as compared to 1.2 mm FWHM for the LabPET8 in iteratively reconstructed images [31]. Animals were imaged at 45 minutes post-injection for a duration of 15 minutes with the head in the center of the field-of-view, then were transferred in the same bed position to the LabPET8/Triumph PET/CT scanner to obtain a CT scan (512 projections, 240 μA, 60 kVp) providing anatomical details. PET data were reconstructed using 20 iterations of a 3D-MLEM algorithm implementing a physical description of the detection process in the system matrix [32].

Image analysis

In patients, regions-of-interest (ROIs) were drawn on clearly assessable foci using the MIM (version 6.0) software. A 2 cm diameter sphere in the frontal right cortex was used as a reference cortical ROI. SUV_{Max} was extracted from the pituitary ROI, whereas the cortical background uptake was based on the SUV_{Mean} value of its corresponding ROI. Pituitary contrast was obtained using the pituitary SUV_{Max} / cortical SUV_{Mean} ratio.

For animal studies, images were analysed with the AMIDE software (version 1.0.4). ROIs were drawn on clearly visualized signals, as well as on a non-specific, 4 × 4 × 1 voxel cortical region of the right frontal cortex. Max count parameter was extracted for discernable foci, and Mean count was used for the cortex ROI, then counts per voxel were converted (using a reference ^{18}F-filled cylindrical phantom) into % injected dose per gram of tissue (%ID/g) by approximating tissue density to 1 g/ml. Contrast values were obtained by dividing the Max count parameter-derived uptake of signal-generating foci by the Mean-calculated %ID/g value of the cortex.

Brain dissection and autoradiography

Immediately after 4FMFES-PET and CT acquisitions, rats imaged on the LabPET II scanner were brought into deep anesthesia (5% isoflurane - 1.5 L/min oxygen). The ribcage was swiftly opened, the abdominal aorta sliced, then the left ventricle was implanted with a needle to systemically perfuse the animal with 500 ml of a 12% paraformaldehyde solution via gravity and heart pumping. After whole-body tissue fixation, the skull was delicately opened, and the brain extracted with the pituitary still lodged inside the *turcica sella*. The decerebrated carcasses and the isolated brains were then sequentially imaged on the LabPET II scanner for 15 minutes each. The brain was then sliced in gross 1-mm-thick slices and placed along the extracted pituitary on an autoradiography phosphor cassette to obtain images of the radiotracer distribution in tissues.

Statistics

Tissue uptake and target-to-cortex ratios for each group were reported as mean ± standard deviation. Sample sizes were arbitrarily chosen since data were retrospectively extracted for the most part from pre-existing studies, but every dataset was considered as following a normal distribution according to a Shapiro-Wilk test, as they were all above the probability threshold set *a priori* at $p = 0.05$. Significance testing between radiotracers was performed using a 1-way ANOVA with Tukey's multiple comparisons test, with a probability threshold set at $p < 0.05$.

Results

Qualitative PET image assessment

In all studied species, and for both FES and 4FMFES, a relatively uniform background-like uptake is observable for most parts of the brain. For rats and mice, a symmetrical, bilateral focus was evident at the base of the midbrain, whereas in humans a single ovoid signal was observed, also at the lower midsection of the brain (Figure 1). In line with previous observations made using FES-PET/MRI image fusion of rat brain [24], scrutinous assessment of FES- and 4FMFES-PET/CT images showed that regardless of the studied species, the strong mid-lower brain signals were localised in the *turcica sella*, which is the anatomical location of the pituitary. Co-injection of 100 μg estradiol in female rats almost abrogated the pituitary signal, showing specific targeting of the tracer (Figure 2).

Another weak and ubiquitous signal anterior to the pituitary, at the base of the brain, was also observable in both rats and mice imaged with either FES or 4FMFES on the LabPET 8/Triumph platform (Figure 3). Imaging in mice and rats following 4FMFES injections using the experimental high-resolution LabPET II scanner enhanced both the pituitary foci and the fainter locus that is anterior to the pituitary, which might have been previously partly obscured because of partial volume effect (Figure 4). This supplemental structure could not be identified precisely with the μCT fusion image, but it could be guessed according to ER expression pattern from previous *ex vivo* FES autoradiography studies that it might be the medial preoptic area (MPOA) [23]. No such signal could be distinguished in the human brain images.

Moreover, strong FES and 4FMFES uptake were observed in the nasal cavity in both mice and rats (Figure 5), but not in humans.

Semi-quantitative PET analysis

The pituitary uptake in tumor-bearing mice reached 1.5 ± 0.3 %ID/g with 4FMFES and 2.8 ± 0.6 %ID/g with FES (Figure 6a), which was even higher than the ER+ tumors that were imaged at the same time. As a comparison, the MC4-L2 tumors implanted in those mice yielded a 4FMFES uptake of 1.7 ± 0.2 %ID/g, which was similar to the pituitary uptake, whereas the FES tumoral uptake of 1.0 ± 0.3 %ID/g was significatively lower than the FES pituitary uptake ($p < 0.001$). However, background signal in the cortex was more than 2-fold lower with 4FMFES compared to FES. As a result, pituitary contrast in mice reached 9.0 ± 2.0 with 4FMFES, even slightly higher than FES contrast (7.9 ± 1.9). Compared to the contrast achieved on MC4-L2 tumors, which was measured as 3.2 ± 0.6 for 4FMFES and 2.3 ± 0.5 for FES, the pituitary contrast was significantly higher for both tracers ($p < 0.001$). The nasal uptake in mice reached 1.0 ± 0.1 %ID/g for FES and 1.1 ± 0.6 %ID/g for 4FMFES.

4FMFES-PET reached higher pituitary uptake than FES-PET in control female rats, with 0.45 ± 0.13 %ID/g and 0.28 ± 0.05 %ID/g ($p < 0.05$), respectively (Figure 6b). Co-injection of excess estradiol with 4FMFES reduced the pituitary uptake down to 0.02 ± 0.01 %ID/g. Since 4FMFES also features a 3-fold lower rat brain background than FES, pituitary contrast was substantially higher (39.3 ± 19.3 and 6.0 ± 1.3 for 4FMFES and FES, respectively; $p < 0.001$). The nasal cavity uptake in rats was measured at 0.10 ± 0.02 %ID/g using FES and at 1.0 ± 0.1 %ID/g with 4FMFES.

In order to mimic pre- and post-menopause conditions in an animal model, ovariectomized rats were compared with a group of intact, control female rats. FES-PET pituitary uptake was significantly higher in ovariectomized rats (0.46 ± 0.11 %ID/g) compared to control animals (0.28 ± 0.05 %ID/g; $p < 0.05$). The use of 4FMFES (0.62 ± 0.27 %ID/g) further enhanced pituitary uptake compared to FES in control animals ($p < 0.05$).

The use of the ultra high-resolution small animal PET platform LabPET II for 4FMFES brain PET imaging in cohorts of mice and rats further amplified the pituitary and postulated MPOA signals compared to the previous generation of scanner (Figure 6a and b). Indeed, significant increases in both pituitary and MPOA measured uptake in mice and rats ($p < 0.001$), and in tissue-to-cortex ratio for mice ($p < 0.005$), were observed with the LabPET II compared to the LabPET8/Triumph platform. A non-significant trend toward higher pituitary- and MPOA-to-cortex ratios was observed in female rats. These data emphasize the importance of high spatial resolution for quantitative assessment of radiotracer uptake in the tiny structures of the brain.

Like what was observed in mice but contrary to the pattern in rats, PET images from patients showed a significantly higher pituitary uptake using FES-PET compared to 4FMFES-PET (SUV_{Max} 1.15 ± 0.22 vs 0.73 ± 0.21, respectively; $p < 0.0001$). However, because the overall brain background is ~2-fold lower with 4FMFES, the pituitary/cortex ratio was higher and a significantly higher contrast was achieved using 4FMFES-PET than FES-PET

(2.61 ± 0.73 vs 2.00 ± 0.47, respectively; $p < 0.01$). Menopausal status did not promote any significant change in pituitary uptake for both tracers. Pre-menopausal women had an average pituitary SUV_{Max} of 1.12 ± 0.20 for FES and of 0.71 ± 0.21 for 4FMFES, whereas post-menopausal patients yielded SUV_{Max} of 1.18 ± 0.22 and 0.76 ± 0.24 for FES and 4FMFES, respectively (Figure 6c).

Dissection and autoradiography

Following careful brain extraction from the small cohort of rats that were injected with 4FMFES, the isolated brain and the remaining carcass (including the pituitary) were imaged by PET imaging (Figure 7a and b). Firstly, images of the remaining carcass centered on the head showed the same strong bilateral signal observed previously, at the position where the pituitary stayed at the bottom of the skull, with a PET uptake of 0.29 ± 0.08 %ID/g, which is similar to the uptake in the live animals.

Secondly, without the surrounding organs and tissues, supplemental signals were evidenced in the isolated brain through PET imaging (Figure 7c). Notably, a single, relatively intense spot in the lower anterior part of the brain could be observed, as well as a set of three foci on the same transverse plane as the pituitary in the central part of the brain. Those signals were reminiscent of previous autoradiography studies [14–17, 23]. Indeed, the location and shape of the foci at the lower part of the brain is similar to the previously described ER distribution in the medial preoptic area (for the anterior signal), and in the arcuate nucleus and the ventromedial nucleus, along with the medial and cortical amygdala for the triple foci situated at the midbrain. Autoradiography of the pituitary along with gross 1 mm-thick slices of the midbrain further supported the findings observed via PET imaging of the isolated brain (Figure 7d).

Discussion

In this work, the distribution pattern and concentration of the ER-targeting PET tracers FES and 4FMFES were observed and analysed in female mice, rats and humans. The most obvious finding across species and common for both tracers is the presence of a strong signal at the base of the skull, co-localized at the *sella turcica*, and consistent with previous reports as being the pituitary [24–25]. The bilateral appearance of the pituitary in rats and in mice is in line with the anatomical arrangement of the ER-rich, horseshoe-shaped adenohypophysis, which flanks the centrally situated but ER-devoid neurohypophysis [33].

Correlative observation between rodent anatomical disposition, brain atlas, ERα brain distribution patterns, autoradiographic studies using radioactive estrogens and FES- and 4FMFES-PET brain PET images of radiotracer uptake were undertaken. It allowed us to hypothesize that the weak PET signal anterior to the pituitary was the ER-rich medial preoptic area (MPOA). Since the MPOA was shown to harbor high ERα expression [14–16, 34] and with the highest *ex vivo* radio-estrogen uptake [17, 23] within the brain (excluding the pituitary), it is indeed very likely that it corresponds to the additional focus observed in PET images. Similarly, the single signal flanked by symmetrical, bilateral foci in the same transverse plane that was only observable in the 4FMFES-PET image of the surgically-removed rat brain and brain slice autoradiography (figure 7c and 7d) are reminiscent of

previous autoradiographic data using radiolabeled estrogens or ERα-specific riboprobe and antibodies [14–17, 23, 34]. Correlating with those studies, it is speculated that those regions are the arcuate and ventromedial nuclei (center), and the medial and cortical amygdala (lateral). Further studies involving histological staining of micrometric slices along with their corresponding 4FMFES autoradiographs would be needed to identify without doubt those structures. Strong FES and 4FMFES uptake were also observed in the nasal cavity of both rats and mice. Since both ERα and β were recently shown to be only weakly expressed in the female mouse nasal epithelium [35], further investigations will be needed in order to elucidate the cause of this uptake.

A trend toward higher pituitary uptake in post-menopausal patients was observed using either tracers, but the difference was not significant. One reason for this might be that not only the pre-menopausal group was substantially smaller (which is expected in a breast cancer cohort), which reduced statistical power, but also menstrual cycle was not taken into account for oncologic PET imaging sessions. However, previous clinical studies already observed that at least for breast cancer tumor uptake, circulating estradiol levels was not a significant confounding factor [36], decreasing the likeliness that FES or 4FMFES pituitary uptake could be significantly influenced by menstrual cycle- or menopause-induced estrogen fluctuations. Nevertheless, the ovariectomy procedure in female rats, which causes more drastic physiological and endocrinal changes than menopause in women, provoked a significant 1.7-fold increase in FES pituitary uptake compared to the control group, a trend that was already observed in previous studies [24]. Whether it is the near-absence of competing physiological estrogens that improved FES binding or an estrogen depletion-induced positive feedback loop triggering pituitary ER overexpression that may explain this increased FES uptake will need to be elucidated in further studies.

Despite lower pituitary 4FMFES uptake in patients, the very low and uniform cerebral background achieved with this tracer allowed the pituitary to be better resolved than with FES. This pattern of better contrast was already exemplified in breast tumors, in which uptake was similar for both tracers but 4FMFES achieved much lower non-specific accumulation, resulting in improved contrast [27]. It was determined in the clinical study that this improved contrast of 4FMFES over FES was mainly due to its 2.5-fold higher resistance to metabolism and to its near-absence of binding to plasma globulins. Both factors contributed to substantially reduce non-specific uptake and blood pool circulating concentration, which in turn reduced the overall background [27]. In rats, 4FMFES yielded better pituitary uptake and contrast than FES, which can be paralleled to the behaviour of those tracers in a previous murine breast cancer study where ER+ tumor uptake and contrast were both significantly improved using 4FMFES [26].

Both FES [37, 38] and 4FMFES [26] were shown to have higher selectivity toward ERα over ERβ, meaning that assessed signals are more likely to originate only from ERα-expressing area of the brain. Imaging of ERβ-rich regions of the brain would necessitate a dedicated PET tracer with high selectivity for this ER isotype, such as 2-[^{18}F]-fluoro-6-(6-hydroxynaphthalen-2-yl)pyridin-3-ol (^{18}F-FHNP) [38].

Despite an ovoid shape, the bilateral distribution of the pituitary was not obvious in humans, which is likely due to the relatively poor spatial resolution of clinical scanners (4.8 mm, 111 μL) compared to our preclinical platforms (LabPET8: ~1.2 mm, 1.7 μL; LabPET II: 0.74 mm, 0.4 μL). In women, the average pituitary volume was reported to range between 460–520 μL, which is 4.1–4.7-fold the volumetric resolution in clinical PET [439]. In comparison, female mice pituitary has a long-axis of 3 mm [40], for a average volume of 6 μL [41], equivalent to ~4 times the volumetric resolution of the LabPET8 scanner, but 15–20 times the volumetric resolution of the LabPET II scanner. Rat PET imaging of the pituitary is benefiting the most from the small animal PET performance, since their average pituitary size is ~100 μL [33], allowing full recovery of the signal with negligible partial volume effect, contrary to clinical imaging of the pituitary in humans and to a less extent in mice, regardless of the preclinical PET system used. Hence, the improved resolution of preclinical PET scanners relative to clinical whole-body PET scanners appears to have more than compensated for the pituitary size difference between humans and rodents.

This is further evidenced with the use of the ultra-high-resolution small animal PET scanner prototype capable of submillimeter volumetric spatial resolution, which allowed even clearer distinction of the bilateral pattern of the foci in both rodent species, as well as enhancing other signals never discerned before by *in vivo* PET imaging. Likewise, better resolution in clinical PET scanners could not only allow to resolve the distinctive bilateral-like shape of human adenohypophysis, but also visualization of additional ER-rich brain structures. The use of dedicated, high-resolution brain PET scanners for humans might enable the investigation of other ERα-rich regions of the brain using 4FMFES. Implementing the LabPET II technology or other high-resolution detection schemes [42,43] in dedicated human brain PET scanners would make spatial resolution down to 1.3 mm (~2 μL) within reach according to Giant4 Application for Tomographic Emission (GATE) simulations [44,45]. Upon completion this would allow to elucidate detailed human ER brain distribution, as well as studying ERα and ERβ fluctuations non-invasively and longitudinally according to age and neuropathological conditions.

One inherent limitation of this study is that the retrospective dataset for mice and patients was optimized for tumor imaging, and as such the brain area was not in the center of the field-of-view for those 2 cohorts, which has slightly impacted image quality in some instances. Another limitation is the lack of fully quantitative and pharmacodynamic data, since cohorts were mostly designed for semi-quantitative assessment of ER+ breast cancer tumors. The systematic combination of every PET acquisition with MRI fusion images, especially in patients, would have allowed more accurate anatomical localization of fine structures and would have enabled anatomy-guided (instead of uptake-guided) ROI drawing. Notwithstanding those considerations, this study still allowed direct comparisons of brain physiological uptake between two different ER-targeting tracers, and across three different species, including humans. Whereas the current technology and investigation tools appear to be suitable to address issues such as the link of pituitary ER-expression to cognitive functions, dedicated ultra-high-resolution brain PET scanners achieving an equivalent resolving power as the available small animal PET imaging technology would be highly desirable to undertake such studies.

Conclusion

The use of FES- and 4FMFES-PET for brain imaging, in dedicated experiments for rats and in collateral retrospective analyses in mice and humans, identified the pituitary as the highest uptake constituent of the brain across species. Another structure, revealed for the first time in PET images of rats and mice, was tentatively attributed to the medial preoptic area of the hypothalamus, in line with previous *ex vivo* observations. Dissection data in rats identified supplemental foci that were reminiscent of the arcuate nucleus, the ventromedial nucleus and the medial and cortical amygdala. Ultra-high resolution 4FMFES brain PET imaging in humans might enable investigation of *in vivo* cerebral ER expression and its role in aging and cognition.

Funding:

This project was indirectly funded by the Canadian Breast Cancer Foundation (CBCF) for the clinical portion, as well as the Natural Sciences and Engineering Research Council of Canada for the development of the scanners. The preclinical studies were carried out with the support of the Sherbrooke Molecular Imaging Center and the Centre de Recherche du Centre Hospitalier Universitaire de Sherbrooke (CRCHUS).

References

1. Muramatsu M, Inoue S (2000) Estrogen receptors: how do they control reproductive and nonreproductive functions? Biochem Biophys Res Commun 270:1–10. [PubMed: 10733896]
2. Shupnik MA (2002) Oestrogen receptors, receptor variants, and oestrogen actions in the hypothalamic-pituitary axis. J Neuroendocrinol 14:85–94. [PubMed: 11849367]
3. Snoeren EM, Antonio-Cabrera E, Spiteri T, et al. (2015) Role of Oestrogen α Receptors in Sociosexual Behaviour in Female Rats Housed in a Seminatural Environment. J Neuroendocrinol 27(11):803–818. [PubMed: 26314929]
4. Balzer BW, Duke SA, Hawke CI, Steinbeck KS (2015) The effects of estradiol on mood and behavior in human female adolescents: a systematic review. Eur J Pediatr 174(3):289–298. [PubMed: 25567794]
5. Mott NN, Pak TR (2013) Estrogen signaling and the aging brain: context-dependent considerations for postmenopausal hormone therapy. ISRN Endocrinol 2013:814690. [PubMed: 23936665]
6. McCarrey AC, Resnick SM (2015) Postmenopausal hormone therapy and cognition. Horm Behav 74:167–172. [PubMed: 25935728]
7. Matyi JM, Rattinger GB, Schwartz S, Buhusi M, Tschanz JT (2019) Lifetime estrogen exposure and cognition in late life: the Cache County Study. Menopause 26(12):1366–1374. [PubMed: 31613825]
8. Farrer LA, Cupples LA, Haines JL, et al. (1997) Effects of age, sex, and ethnicity on the association between apolipoprotein E genotype and Alzheimer disease: a meta-analysis. JAMA 278:1349–1356. [PubMed: 9343467]
9. Brinton RD, Yao J, Yin F, Mack WJ, Cadenas E (2015) Perimenopause as a neurological transition state. Nat Rev Endocrinol 11:393–405. [PubMed: 26007613]
10. Rocca WA, Grossardt BR, Shuster LT (2014) Oophorectomy, estrogen, and dementia: A 2014 update. Mol Cell Endocrinol 389:7–12. [PubMed: 24508665]
11. Espeland MA, Shumaker SA, Leng I, et al. (2013) Long-term effects on cognitive function of postmenopausal hormone therapy prescribed to women aged 50 to 55 years. JAMA Intern Med 173(15):1429–1436. [PubMed: 23797469]
12. Wharton W, Gleason CE, Dowling NM, et al. (2014) The KEEPS-Cognitive and Affective Study: baseline associations between vascular risk factors and cognition. J Alzheimers Dis 40(2):331–341. [PubMed: 24430001]
13. Humphreys GI, Ziegler YS, Nardulli AM (2014) 17β-Estradiol Modulates Gene Expression in the Female Mouse Cerebral Cortex. PLOS One 9(11):e111975. [PubMed: 25372139]

14. Mahfouz A, Lelieveldt BP, Grefhorst A, et al. (2016) Genome-wide coexpression of steroid receptors in the mouse brain: Identifying signaling pathways and functionally coordinated regions. Proc Natl Acad Sci USA 113(10):2738–2743. [PubMed: 26811448]
15. Shughrue PJ, Lane MV, Merchenthaler I (1997) Comparative distribution of estrogen receptor-alpha and -beta mRNA in the rat central nervous system. J Comp Neurol 388(4):507–525. [PubMed: 9388012]
16. Mitra SW, Hoskin E, Yudkovitz J, et al. (2003) Immunolocalization of estrogen receptor beta in the mouse brain: comparison with estrogen receptor alpha. Endocrinology 144(5):2055–2067. [PubMed: 12697714]
17. Merchenthaler I, Lane MV, Numan S, Dellovade TL (2004) Distribution of estrogen receptor alpha and beta in the mouse central nervous system: in vivo autoradiographic and immunocytochemical analyses. J Comp Neurol 473(2):270–291. [PubMed: 15101093]
18. Kiesewetter DO, Kilbourn MR, Landvatter SW, et al. (1984) Preparation of four fluorine- 18-labeled estrogens and their selective uptakes in target tissues of immature rats. J Nucl Med 25(11):1212–1221. [PubMed: 6092569]
19. Seimbille Y, Rousseau J, Bénard F, et al. (2002) ^{18}F-labeled difluoroestradiols: preparation and preclinical evaluation as estrogen receptor-binding radiopharmaceuticals. Steroids 67(9):765–775. [PubMed: 12123788]
20. Fowler AM, Chan SR, Sharp TL, et al. (2012) Small-animal PET of steroid hormone receptors predicts tumor response to endocrine therapy using a preclinical model of breast cancer. J Nucl Med 53(7):1119–1126. [PubMed: 22669982]
21. Wang Y, Ayres KL, Goldman DA, et al. (2017) 18F-Fluoroestradiol PET/CT Measurement of Estrogen Receptor Suppression during a Phase I Trial of the Novel Estrogen Receptor-Targeted Therapeutic GDC-0810: Using an Imaging Biomarker to Guide Drug Dosage in Subsequent Trials. Clin Cancer Res 23(12):3053–3060. [PubMed: 28011460]
22. Chae SY, Ahn SH, Kim SB, et al. (2019) Diagnostic accuracy and safety of 16α-[18F]fluoro-17β-oestradiol PET-CT for the assessment of oestrogen receptor status in recurrent or metastatic lesions in patients with breast cancer: a prospective cohort study. Lancet Oncol 20(4):546–555. [PubMed: 30846327]
23. Pareto D, Alvarado M, Hanrahan SM, Biegon A (2004) In vivo occupancy of female rat brain estrogen receptors by 17beta-estradiol and tamoxifen. Neuroimage 23(3):1161–1167. [PubMed: 15528115]
24. Khayum MA, de Vries EF, Glaudemans AW, Dierckx RA, Doorduin J (2014) In vivo imaging of brain estrogen receptors in rats: a 16α−^{18}F-fluoro-17β-estradiol PET study. J Nucl Med 55(3):481–487. [PubMed: 24481026]
25. Moresco RM, Casati R, Lucignani G, et al. (1995) Systemic and cerebral kinetics of 16 alpha [^{18}F]fluoro-17 beta-estradiol: a ligand for the in vivo assessment of estrogen receptor binding parameters. J Cereb Blood Flow Metab 15(2):301–311. [PubMed: 7860663]
26. Paquette M, Phoenix S, Ouellet R, et al. (2013) Assessment of the novel estrogen receptor PET tracer 4-fluoro-11β-methoxy-16α-[(18)F]fluoroestradiol (4FMFES) by PET imaging in a breast cancer murine model. Mol Imaging Biol 15(5):625–632. [PubMed: 23619898]
27. Paquette M, Lavallée É, Phoenix S, et al. (2018) Improved Estrogen Receptor Assessment by PET Using the Novel Radiotracer ^{18}F-4FMFES in Estrogen Receptor-Positive Breast Cancer Patients: An Ongoing Phase II Clinical Trial. J Nucl Med 59(2):197–203. [PubMed: 28798032]
28. Gaudin E, Thibaudeau C, Arpin L, et al. (2017) Initial results of a truly pixelated APD-based PET scanner for high-resolution preclinical imaging. J Nucl Med 58 (suppl 1): 91. [PubMed: 27516446]
29. Lim JL, Zheng L, Berridge MS, Tewson TJ (1996) The use of 3-methoxymethyl-16-beta, 17-beta-epiestriol-O-cyclic sulfone as the precursor in the synthesis of [^{18}F]-16α-fluoroestradiol. Nucl Med Biol 23:911–915. [PubMed: 8971859]
30. Seimbille Y, Ali H, van Lier JE (2002) Synthesis of 2,16α- and 4,16α-difluoroestradiols and their 11β-methoxy derivatives as potential estrogen receptor-binding radiopharmaceuticals. J Chem Soc Perkin Trans 5:657–663.

31. Bergeron M, Cadorette J, Tétrault MA, et al. (2014) Imaging performance of LabPET APD-based digital PET scanners for pre-clinical research. Phys Med Biol 59(3):661–678. [PubMed: 24442278]
32. Selivanov VV, Picard Y, Cadorette J, Rodrigue S, Lecomte R (2000) Detector response models for statistical iterative image reconstruction in high resolution PET. IEEE Trans Nucl Sci 47(3):1168–1175.
33. Mitchner NA, Garlick C, Ben-Jonathan N (1998) Cellular distribution and gene regulation of estrogen receptors alpha and beta in the rat pituitary gland. Endocrinology 139(9):3976–3983. [PubMed: 9724053]
34. Laflamme N, Nappi RE, Drolet G, Labrie C, Rivest S (1998) Expression and neuropeptidergic characterization of estrogen receptors (ERα and ERβ) throughout the rat brain: anatomical evidence of distinct roles of each subtype. J Neurobiol 36: 357–378. [PubMed: 9733072]
35. Kanageswaran N, Nagel M, Scholz P, Mohrhardt J, Gisselmann G, Hatt H (2016) Modulatory effects of sex steroids progesterone and estradiol on odorant evoked responses in olfactory receptor neurons. PLoS One. 2016;11(8):e0159640. [PubMed: 27494699]
36. Peterson LM, Kurland BF, Linka JM, et al. (2011) Factors influencing the uptake of 18F-fluoroestradiol in patients with estrogen receptor positive breast cancer. Nucl Med Biol 38:969–978. [PubMed: 21982568]
37. Yoo J, Dence CS, Sharp TL, Katzenellenbogen JA, Welch MJ (2005) Synthesis of an estrogen receptor-β selective radioligand: 5-[^{18}F]fluoro-(2R*,3S*)-2,3-bis(4-hydroxyphenyl)pentanenitrile and comparison of in vivo distribution with 16α-[^{18}F]Fluoro-17β-estradiol. J Med Chem 48:6366–6378. [PubMed: 16190762]
38. Antunes IF, van Waarde A, Dierckx RA, et al. (2017) Synthesis and Evaluation of the Estrogen Receptor β-Selective Radioligand 2–18F-Fluoro-6-(6-Hydroxynaphthalen-2-yl)Pyridin-3-ol: Comparison with 16α−18F-Fluoro-17β-Estradiol. J Nucl Med 58(4):554–559. [PubMed: 27908969]
39. Lamichhane TR, Pangeni S, Paudel S, Lamichhane HP (2015) Age and gender related variations of pituitary gland size of healthy nepalese people using magnetic resonance imaging. Am J Biomed Eng 5(4):130–135.
40. Cao D, Ma X, Zhang WJ, Xie Z (2017) Dissection and Coronal Slice Preparation of Developing Mouse Pituitary Gland. J Vis Exp 16(129) doi: 10.3791/56356.
41. DuBray La Perle KM, Dintzis SM (2017) Endocrine System. In: Treuting PM, Dintzis SM, Montine KS (eds). Comparative Anatomy and Histology; a Mouse, Rat and Human Atlas. Elsevier, p. 251–273.
42. Catana C (2019) Development of dedicated brain PET imaging devices: recent advances and future perspectives. J Nucl Med 60(8):1044–1052. [PubMed: 31028166]
43. Watanabe M, Saito A, Isobe T, et al. (2017) Performance evaluation of a high-resolution brain PET scanner using four-layer MPPC DOI detectors. Phys Med Biol 62(17):7148–7166. [PubMed: 28753133]
44. Gaudin É, Toussaint M, Thibaudeau C, et al. (2019) Performance Simulation of an Ultra-High Resolution Brain PET Scanner Using 1.2-mm Pixel Detectors. IEEE Trans Radiat Plasma Med Sci 3(3):334–342. [PubMed: 31453423]
45. Gaudin É, Toussaint M, Thibaudeau C, et al. (2019) Simulation Studies of the SAVANT High Resolution Dedicated Brain PET Scanner Using Individually Coupled APD Detectors and DOI Encoding. J Nucl Med 60 (suppl 1):531.

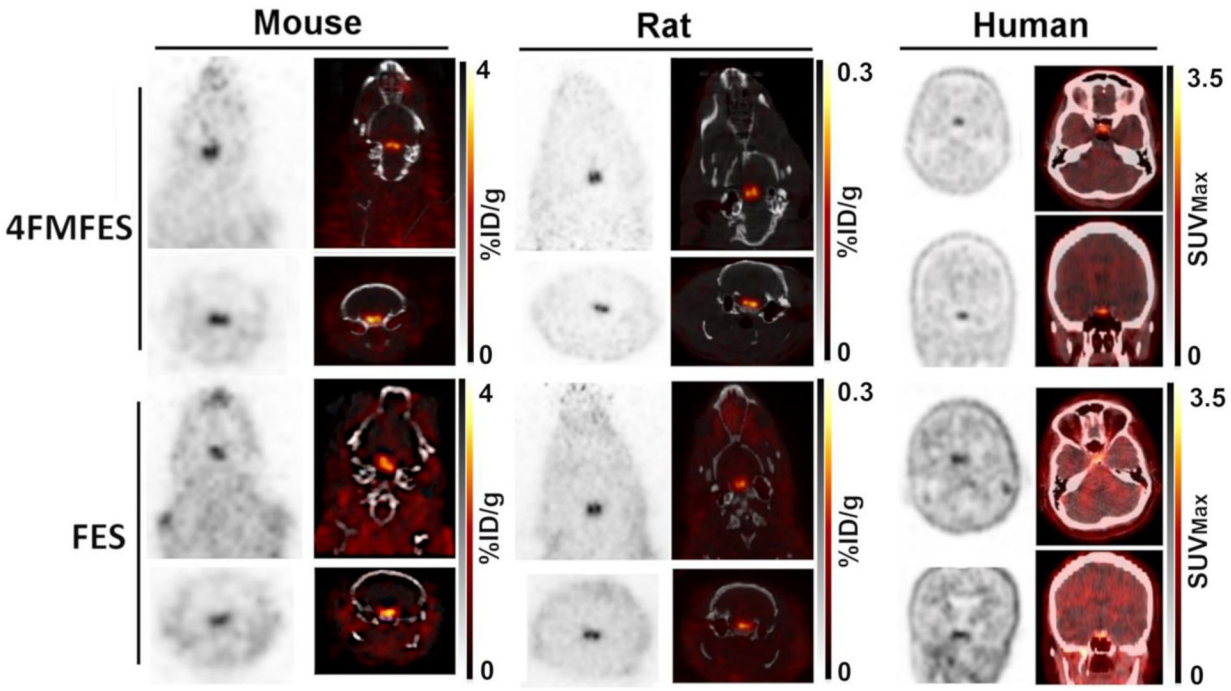

Figure 1: Cross-species 4FMFES- and FES-PET brain imaging.

Representative coronal and transaxial images of brain slices from 4FMFES and FES PET/CT for mouse (left panels), rat (middle panels) and human (right panels), all centered on the pituitary. The patient shown was a 57 years-old post-menopausal woman. The grayscale (PET) and hot metal scale (PET component in the PET/CT fusion images) uptake values are indicated for each dataset in %ID/g for animal studies and in SUV_{Max} for clinical images. Rodent images were obtained on the LabPET8/Triumph preclinical PET/CT platform. Clinical images were obtained on a Philips TF whole-body PET/CT scanner.

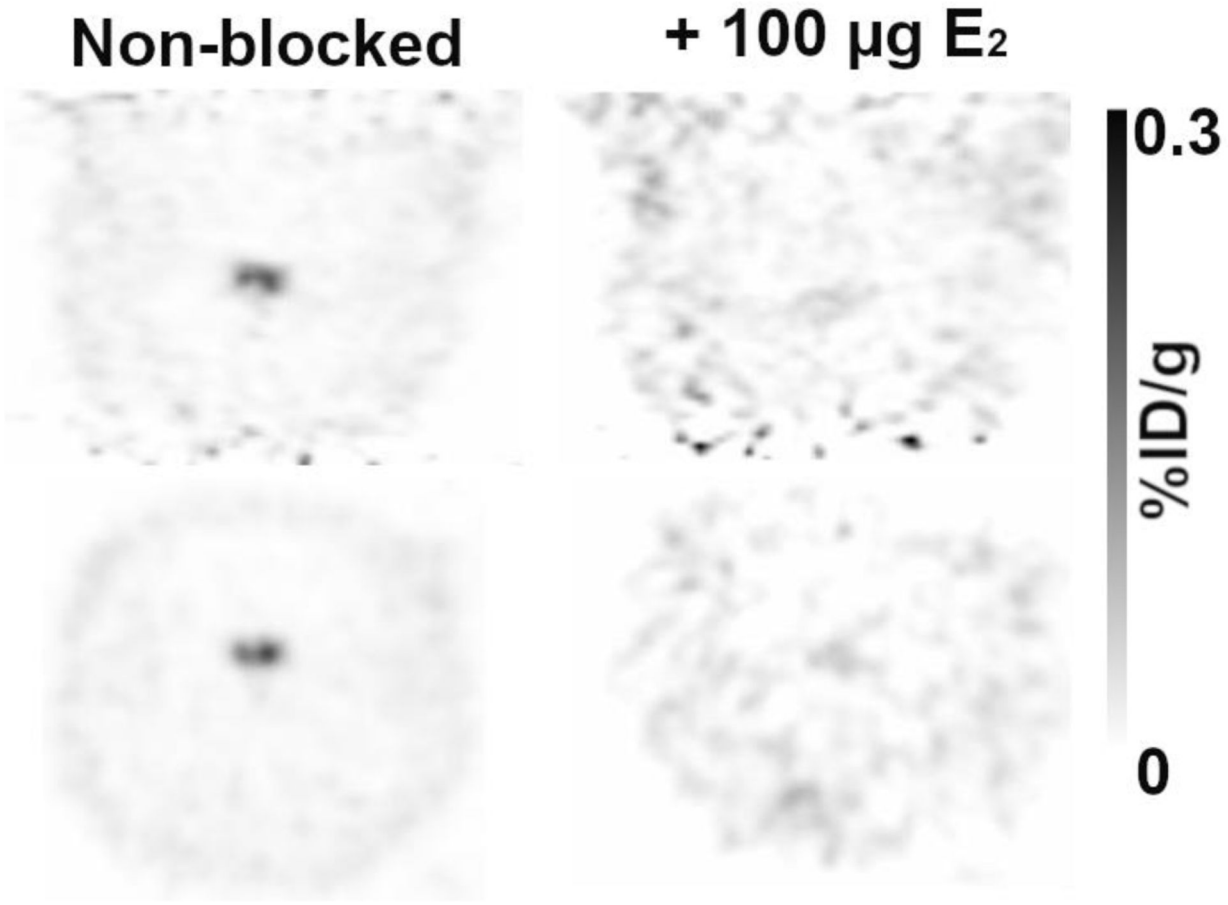

Figure 2:

Coronal (top) and transaxial (bottom) views of 4FMFES-PET images centered on the pituitary without (left) or with (right) co-injection of 100 µg estradiol (E_2). Scans were performed one week apart. Co-injection of E_2 with 4FMFES provoked a 25-fold decrease in signal intensity, almost down to cortical levels. Intensity scale in %ID/g in grayscale is the same for both images.

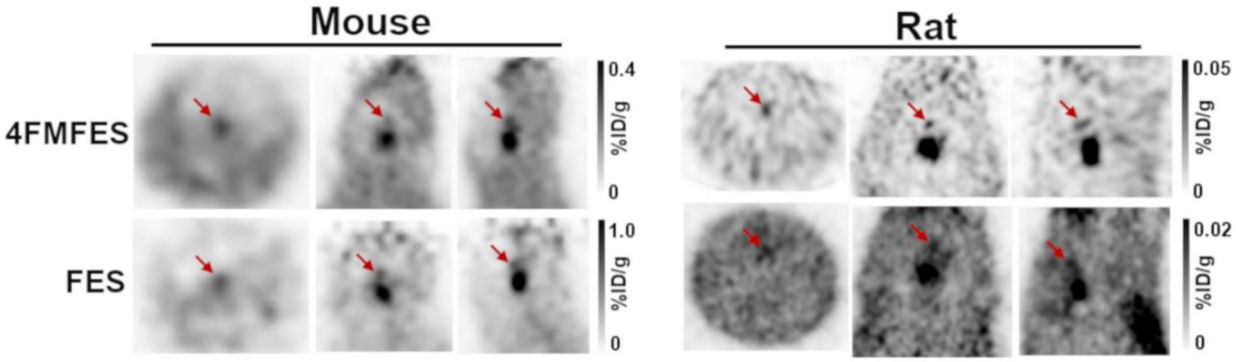

Figure 3:

Orthogonal 4FMFES and FES-PET views centered on the MPOA (red arrows) in female mice and in rats using the LabPET 8/Triumph platform. Signals are relatively faint and hard to evidence, especially in mice. Intensity scales in %ID/g in grayscale are displayed for each dataset.

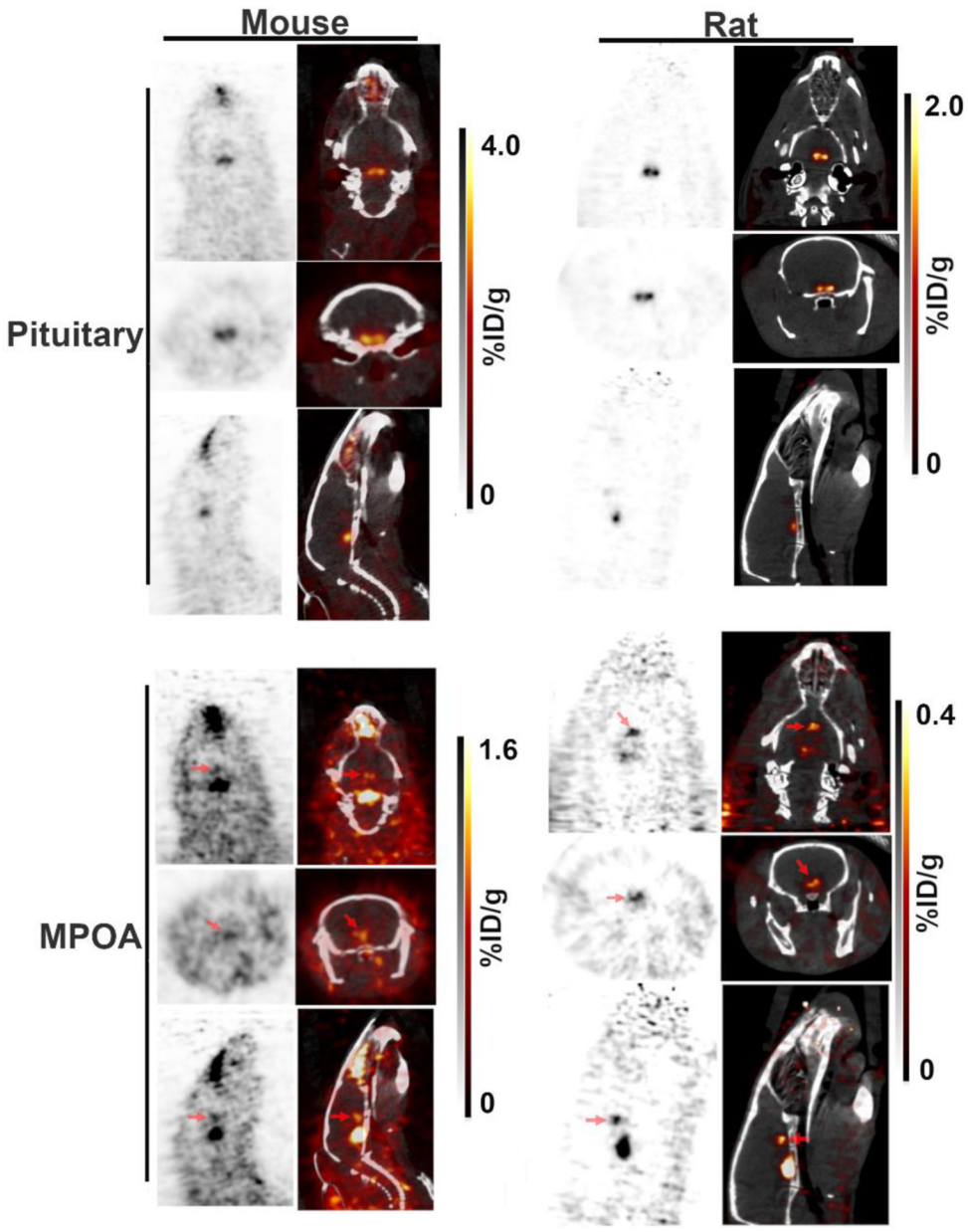

Figure 4: Sub-millimetric resolution 4FMFES-PET and PET/CT images of mouse and rat brains.

The bilateral aspect of the pituitary was better resolved using the prototypical LabPET II preclinical scanner (FWMH = 0.74 mm) in both mice and rats pre-injected with 4FMFES (top panels). Furthermore, the supplemental signal anterior to the pituitary likely to be the ER-rich medial preoptic area (MPOA; bottom panels) was better visualized in the mouse and rat brains (red arrows) than with the LabPET 8/Triumph scanner. The grayscale (PET) and hot metal scale (PET component in the PET/CT fusion images) uptake values are indicated for each dataset in %ID/g.

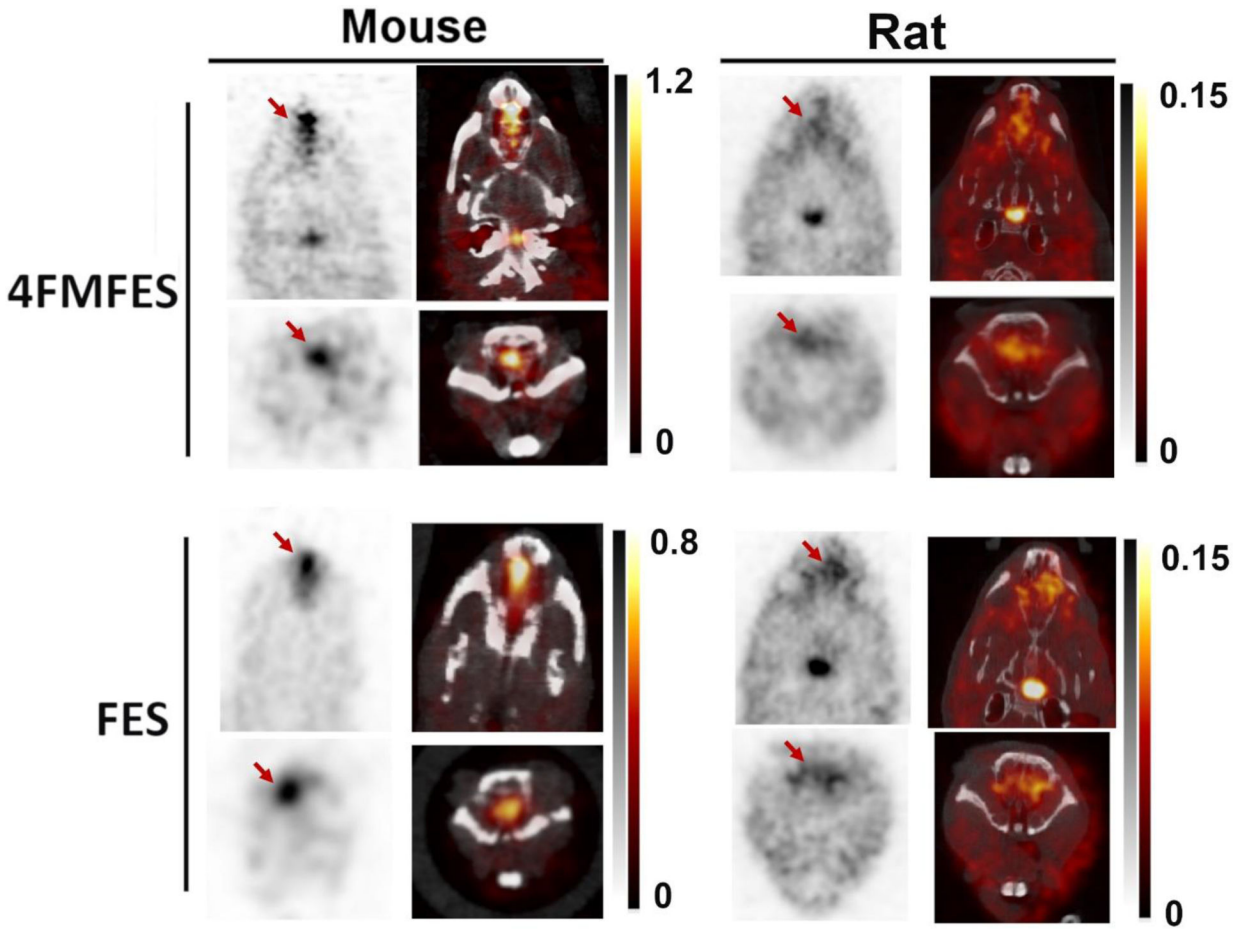

Figure 5:
Nasal uptake (red arrows) in female mice and rats imaged with FES and 4FMFES-PET and PET/CT. The signal is more intense in mice than in rats, and similar between 4FMFES and FES in the same species. No equivalent uptake was observed in the breast cancer patient cohort. Intensity scales in %ID/g in both grayscale (PET) and hot metal (PET/CT) are displayed for each dataset.

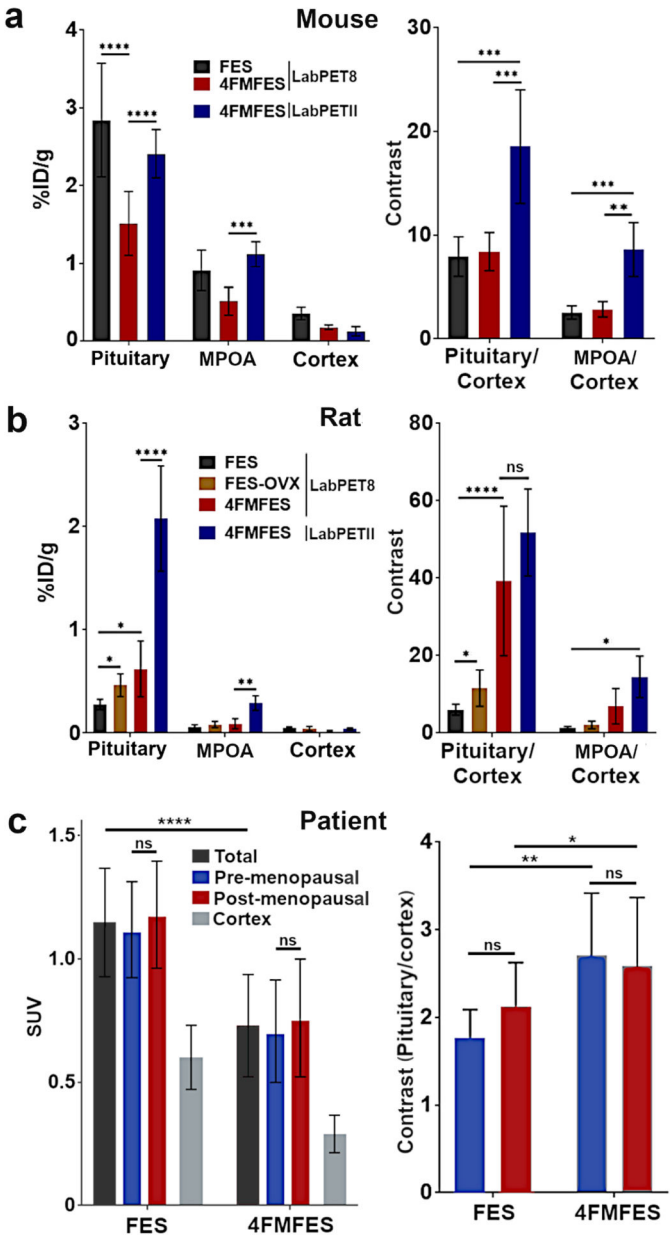

Figure 6: Cross-species semi-quantitative uptake (left panels) and contrast (right panels) values of FES and 4FMFES brain PET images.

a) FES or 4FMFES uptake and contrast in the pituitary, the newly identified anterior signal attributed to the medial preoptic area (MPOA) and the cortex of mice. While 4FMFES specific uptake is lower than with FES, cortical background is also much lower. The use of the high-resolution LabPET II scanner increased the pituitary and anterior 4FMFES measured uptake values ~1.5-fold. Pituitary- and MPOA-to-cortex contrast was similar for both FES and 4FMFES, with a 2-fold increase for 4FMFES using the LabPET II scanner. **b)** FES and 4FMFES uptake in control and ovariectomized (OVX) female rats. Significantly higher pituitary FES uptake was observed in OVX rats compared to the control group. Pituitary 4FMFES uptake in normal female rats was higher than FES uptake, with a lower cortical accumulation. The LabPET II platform after injection of 4FMFES further increased

the measured pituitary and MPOA uptake 3-fold. Pituitary- and MPOA-to-cortex contrast increases progressively for FES (control), FES-OVX, 4FMFES and 4FMFES with the LabPET II scan. **c)** Pituitary uptake in women was higher using FES by almost a factor of two compared to 4FMFES. No differences in uptake or pituitary-to-cortex contrast were observed between pre- or post-menopausal women for both tracers. Brain background was 2-fold lower with 4FMFES resulting in a better contrast compared to FES despite the lower pituitary uptake. *: $p < 0.05$; **: $p < 0.01$; ***: $p < 0.005$; ****: $p < 0.001$

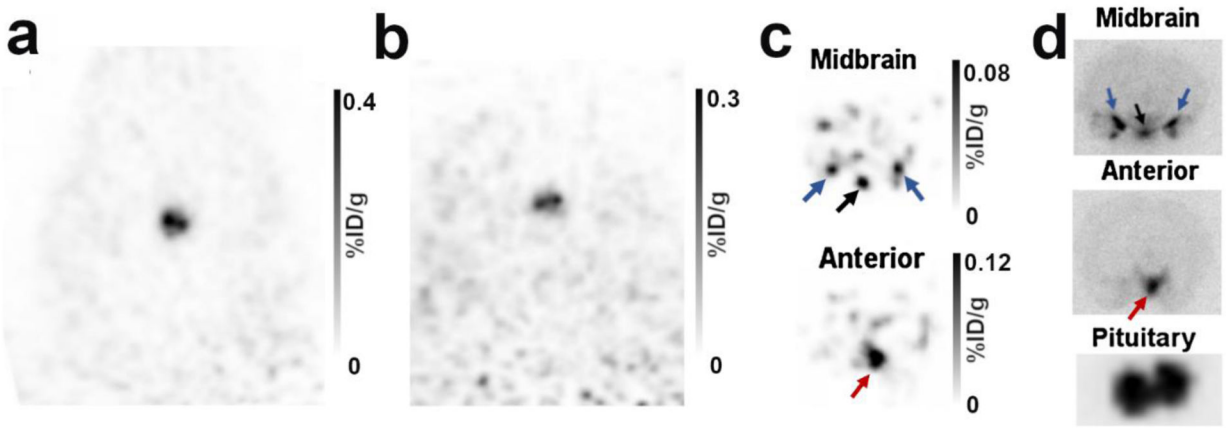

Figure 7: Dissected brain images following 4FMFES injection in female rats.

a) Typical coronal views of the pituitary of a live female rat 1 hour following injection of 4FMFES. **b)** After removal of the brain immediately after the *in vivo* PET scan, the pituitary stem remained in the skull. PET imaging of the brainless carcass reproduced the same bilateral signal as in the live animals, confirming that the signal originated from the pituitary. **c)** PET image of the isolated brain. A transverse midbrain slice aligned with the pituitary revealed 3 foci at the bottom of the brain which are likely to be the arcuate and ventromedial nuclei (black arrows), along with the medial and cortical amygdala (blue arrows). A transverse slice situated ~3 mm anterior to the "midbrain" slice reproduced the weak anterior signal (red arrows) seen in figure 3 and 4, which correspond to the medial preoptic area (MPOA). **d)** Autoradiography of 1 mm thick slices of the regions revealed in (c) and of the isolated pituitary.